

## The Effect of One Valence Electron: Contrasting (PNP)Ni(CO) with (PNP)Ni(NO) to Understand the Half-Bent NiNO Unit

Benjamin C. Fullmer, Maren Pink, Hongjun Fan, Xiaofan Yang, Mu-Hyun Baik,\* and Kenneth G. Caulton\*

Department of Chemistry, Indiana University, Bloomington, Indiana 47405

Received December 27, 2007

Reaction of a (PNP)Ni radical with NO finishes in the time of mixing to form a 1:1 adduct with a NO stretching frequency of 1654 cm<sup>-1</sup>. NMR data of this diamagnetic product indicate C<sub>2v</sub> symmetry, which is contradicted by the X-ray structure, which shows it to be nonplanar at Ni, with a geometry intermediate between planar and tetrahedral; the planar geometry is thus the transition state for fluxionality giving time-averaged C<sub>2v</sub> symmetry. The X-ray structure, together with DFT calculations, reveals that the “half-bent” NiNO unit and the intermediate coordination geometry result from a Ni → NO charge transfer, which has a nonintegral value, resulting in a continuum between NO<sup>+</sup> (hence Ni<sup>0</sup>) and NO<sup>-</sup> (hence Ni<sup>II</sup>). This is related to the nonaxially symmetric character of the Ni → NO back-donation caused by the (PNP) environment on Ni. Steric effects of <sup>t</sup>Bu and even chelate constraints are ruled out as the cause of the unusual electronic and structural features.

### Introduction

The effect of a single electron transfer on structure, bonding, and ligand binding thermodynamics is one of the simplest changes and thus is anticipated to be one subject to prediction. The pair to be compared is most often compositionally identical but different by a one-electron redox change (e.g., Co(NH<sub>3</sub>)<sub>6</sub><sup>n+</sup>, *n* = 2 or 3). Another pair can be periodic table neighbors: M(H<sub>2</sub>O)<sub>6</sub><sup>+2</sup> for M = Mn and Fe, where an accompanying change is the number of nuclear protons and (one) electron. In this study, we make an analogous comparison, but one electron and one nuclear proton are added not to the metal but to the carbon of NiCO<sup>+</sup> to yield NiNO<sup>+</sup>. The odd-electron change means that the 18-electron rule has little or no predictive character in this case.<sup>1</sup> In addition, the electronic structure of the {MNO} configuration<sup>2</sup> discussed in this work is poorly understood.<sup>3</sup> Regarding structural precedent, most structures of NiL<sub>2</sub>(X)-(NO) suffer from disorder,<sup>4,5</sup> which limits the structural

generalization: Ni nonplanar with (highly variable) bent NiNO. Exceptions involve three MeC(CH<sub>2</sub>O)<sub>3</sub>P ligands on (NiNO)<sup>+</sup>, which is pseudotetrahedral with linear NiNO and several recently reported<sup>6–8</sup> structures.

We have already reported<sup>9</sup> that spin doublet, unsaturated, T-shaped (PNP)Ni<sup>I</sup> will bind one molecule of CO and establish a fully reversible equilibrium. This represents a 15/17-electron reagent forming a 17/19-electron product, the difference between the paired numbers being whether or not the amide nitrogen donates its p<sub>π</sub> lone pair to nickel. The carbonylation is completely reversible in that (PNP)Ni can be recovered easily under a vacuum, which is very unusual for a ligand as strong as CO. This finding was echoed by a weak Ni–CO binding enthalpy of –8.3 kcal/mol calculated by DFT(B3LYP), comparable<sup>10</sup> to TΔS at 298 K. The geometric structure of d<sup>9</sup> (PNP)Ni(CO) is flattened tetrahedral, as shown in Figure 1, quite unlike that of planar d<sup>8</sup> (PNP)Co(CO), a consequence attributed to rehybridization of the semioccupied molecular orbital (SOMO) of planar (PNP)Ni with its 4p<sub>z</sub> lowest unoccupied molecular orbital (LUMO)

\* Author to whom correspondence should be addressed. E-mail: caulton@indiana.edu (K.G.C.).

- (1) Xu, N.; Powell, D. R.; Cheng, L.; Richter-Addo, G. B. *Chem. Commun.* **2006**, 2030.
- (2) Enemark, J. H.; Feltham, R. D. *Coord. Chem. Rev.* **1974**, *13*, 339.
- (3) Ara, I.; Fornies, J.; Garcia-Monforte, M. A.; Menjon, B.; Sanz-Carrillo, R. M.; Tomas, M.; Tsipis, A. C.; Tsipis, C. A. *Chem.—Eur. J.* **2003**, *9*, 4094.
- (4) Enemark, J. H. *Inorg. Chem.* **1971**, *10*, 1952.
- (5) Haller, K. J.; Enemark, J. H. *Inorg. Chem.* **1978**, *17*, 3552.

- (6) Iluc, V. M.; Miller, A. J. M.; Hillhouse, G. L. *Chem. Commun.* **2005**, 5091.

- (7) Landry, V. K.; Pang, K.; Quan, S. M.; Parkin, G. *Dalton Trans.* **2007**, 820.

- (8) Landry, V. K.; Parkin, G. *Polyhedron* **2007**, *26*, 4751.

- (9) Ingleson, M. J.; Fullmer, B. C.; Buschhorn, D. T.; Fan, H.; Pink, M.; Huffman, J. C.; Caulton, K. G. *Inorg. Chem.* **2008**, *47*, 407.

- (10) Watson, L. A.; Eisenstein, O. *J. Chem. Educ.* **2002**, *79*, 1269.

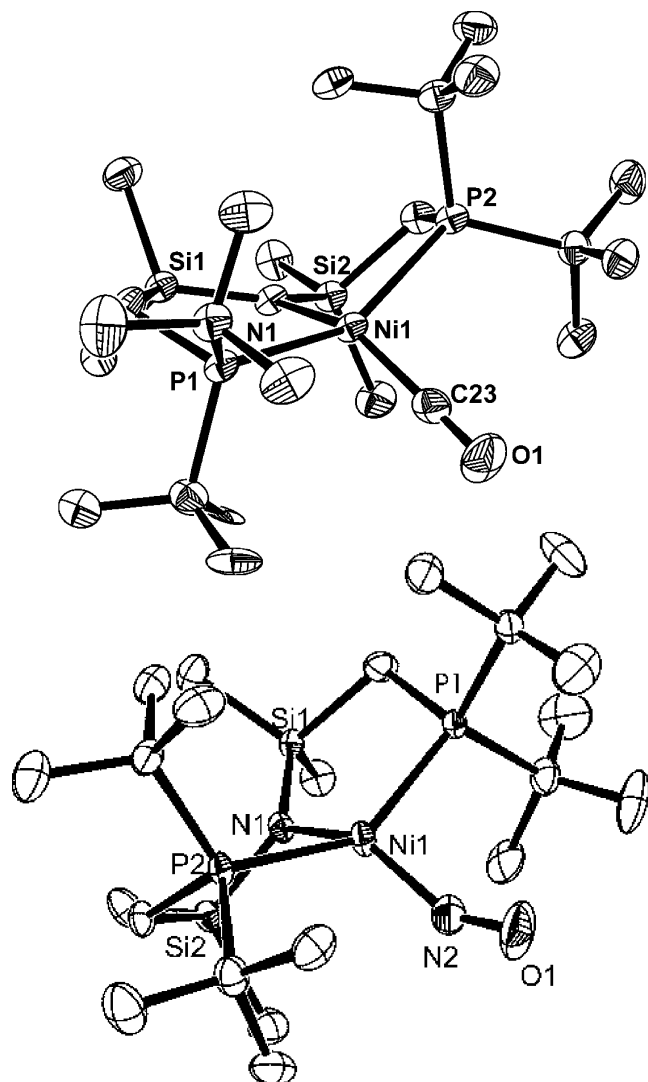
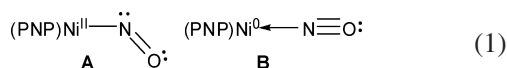


**Figure 1.** Above: ORTEP drawing of (PNP)Ni(CO). Below: ORTEP drawing (50% probabilities) of the non-hydrogen atoms of (PNP)Ni(NO), showing selected atom labelling. Unlabeled atoms are carbons. Selected structural parameters: Ni–N2 1.692(4) Å; Ni–N1, 2.014(4) Å; Ni–P1, 2.2604(13) Å; Ni–P2, 2.3422(13) Å; N2–O1, 1.185(5) Å;  $\angle$ N1–Ni–N2, 140.40(18)°; P1–Ni–P2, 143.21(5)°; N2–Ni–P1, 100.78(14)°; N2–Ni–P2, 103.52(14)°; Ni–N2–O1, 149.3(4)°.

to give two orbitals, one being the SOMO and the second accepting the CO lone pair. What structure is expected for (PNP)Ni(NO)? Radical (PNP)Ni would appear to be an ideal reaction partner for radical NO,<sup>11,12</sup> since structure **A** (eq 1) gives a coupling product (R–NO analog).



More specifically, the SOMO of (PNP)Ni has  $\sigma$  symmetry (see below) and is directed opposite the SiN<sub>2</sub>N–Ni bond and should promote good radical/radical coupling and create Ni<sup>II</sup>. In other words, if NO approaches in a bent geometry as a Lewis base (N lone pair), the LUMO of (PNP)Ni is mainly of 4p<sub>z</sub> character, perpendicular to the NP<sub>2</sub>Ni plane,

and can bind NO by the nitrogen lone pair and simultaneously initiate electron transfer to the  $\pi_{\text{NO}}^*$  from Ni. Since bent NO (i.e., NO<sup>-</sup>) binds analogously to hydride, halide, or hydrocarbyl, this yields Ni<sup>II</sup> and thus predicts a planar coordination geometry labeled **A** in eq 1. If, on the other hand, arriving NO effects a one-electron reduction of Ni<sup>I</sup>, the resulting linear Ni<sup>0</sup>(NO<sup>+</sup>) unit, **B**, should have a tetrahedral structure (compare<sup>13</sup> linear NiNO in C<sub>3v</sub> symmetric (MeC(CH<sub>2</sub>O)<sub>3</sub>P)<sub>3</sub>Ni(NO)<sup>+</sup>); a nonplanar geometry will of course be resisted by the ring constraints of  $\eta^3$ -(PNP) on nickel.

## Results

Reaction of (PNP)Ni with substoichiometric NO in arene solvents is complete in the time of mixing at and below 23 °C to give a 1:1 adduct that is unchanged by vacuum drying, unlike the carbonyl analog. The <sup>1</sup>H ('Bu, one CH<sub>2</sub>, and one SiMe) and <sup>31</sup>P (single chemical shift) NMR spectra of this (PNP)Ni(NO) in benzene indicates C<sub>2v</sub> molecular symmetry and diamagnetic behavior; in conflict with this symmetry is the fact that there is no virtual coupling in the 'Bu <sup>1</sup>H NMR resonance (they are simple doublets, suggesting  $\angle$ P–Ni–P much below 180°). The  $\nu_{\text{NO}}$  value of this product, 1654 cm<sup>-1</sup>, is the lowest reported value for a nickel nitrosyl, but it does not uniquely distinguish between linear and bent NiNO structures. Structure determination by X-ray diffraction was initially plagued by (a) the characteristic reactivity of violet (PNP)Ni(NO) to be oxidized by NO to give orange (PNP)Ni(ONO) and (b) the characteristic behavior of (PNP)Ni(NO) to cocrystallize with either (PNP)Ni(ONO), or (PNP)Ni when substoichiometric NO was employed. Figure 1 shows the structure of (PNP)Ni(NO) from a crystal that contained no second species (see the Experimental Section). The crystals of (PNP)Ni(EO), E = C and N, are crystallographically isomorphous, and the molecules have remarkably similar<sup>14</sup> structures: a flattened tetrahedral coordination geometry halfway between planar and tetrahedral with consequent distortion of the two fused five-membered chelate rings to becoming inequivalent. Consequently, the Ni–P distances are different by as much as 0.08 Å. There are no major differences in the Ni–NSi<sub>2</sub> distances; no agostic interactions to methyl of 'Bu or Si are found, and the single largest difference is the Ni–E–O angle, essentially linear at 175.6(4)° for the carbonyl and bent for the nitrosyl at 149.3(4)°. Since these differences exist in the same crystal packing environment, they must be due to electronic preferences intrinsic to the single molecular species, not to distorting forces of the lattice.

In the choice between linear NO<sup>+</sup> (hence tetrahedral Ni<sup>0</sup>) and bent NO<sup>-</sup> (Ni<sup>II</sup>), the molecule chooses the intermediate case, judging by the Ni–N–O angle, which should be near 125–130° for true NO<sup>-</sup>. The observed angle Ni–N–O of 140–150° we term “half-bent.” The coordination geometry of the carbonyl shows that P<sub>2</sub>NNi nonplanarity is already

(11) Ford, P. C.; Lorkovic, I. M. *Chem. Rev. (Washington, DC)* **2002**, *102*, 993.

(12) McCleverty, J. A. *Chem. Rev. (Washington, DC, U.S.A.)* **2004**, *104*, 403.

(13) Meiners, J. H.; Rix, C. J.; Clardy, J. C.; Verkade, J. G. *Inorg. Chem.* **1975**, *14*, 705.

(14) See the Supporting Information.

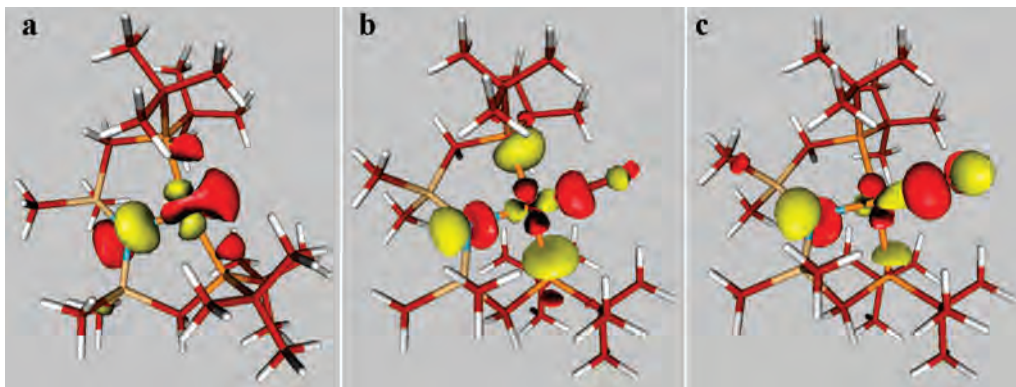


**Figure 2.** Orbital contour diagrams of (a) the SOMO of (PNP)Ni, (b) the SOMO of (PNP)Ni(CO), and (c) the HOMO of (PNP)Ni(NO), each at its equilibrium geometry.

established at the  $d^9$  configuration, so that is not related to the one  $e^-$  change on going to  $\{\text{NiNO}\}^{10}$ . The near-identical  $t\text{Bu}$  conformations and identical solid state packing for  $E = \text{C}$  and  $\text{N}$  suggest that the different bending is caused by intramolecular electronic effects, not by steric conflicts. In summary, these observations establish that the most salient effect of conversion of  $\text{C}$  to  $\text{N}$  in (PNP)Ni(EO) is bending of the NiEO substructure. This finding is in disagreement with the  $C_{2v}$  symmetry indicated by the NMR data, however, and implies that conversion between the two enantiomers (i.e., two P bent “up” vs “down”) via a planar transition state must be a facile process at room temperature and places the transition state energetically within  $\sim 15$  kcal/mol of the ground state. For comparison, the optimized DFT(B3LYP) geometry of (PNP)Ni(NO) with the NiNO angle constrained to  $180^\circ$  lies 5.8 kcal/mol higher than the bent form but still has a flattened tetrahedral structure, with trans angles  $132^\circ \pm 1^\circ$ .

Why is the NiNO angle “half-bent”, and why are the concepts of formal oxidation state applicable to nickel in (PNP)Ni(NO)?

### Computational Analysis

**a. (PNP)Ni(EO) Species.** DFT calculations were employed to understand how formally adding one nuclear proton and one electron to the carbon of flattened tetrahedral (PNP)Ni(CO) results in “half-bending” of the Ni–E–O angle. DFT calculations at the B3LYP/6-31G\*\* level successfully capture the key observed geometric changes from carbonyl to nitrosyl: both have intermediate, that is, non-planar, coordination geometries, but the carbonyl is nearly linear with a Ni–C–O angle of  $174.6^\circ$ , while the nitrosyl is bent with a computed Ni–N–O angle of  $146.8^\circ$ . Also consistent with experiment is that the binding enthalpy of NO to (PNP)Ni of 15.4 kcal/mol is nearly twice that of CO. The composition of the SOMO of (PNP)Ni(CO) shown in Figure 2 is  $\sigma$ -antibonding between Ni and both P and  $\text{NSi}_2$ . This calculated involvement of phosphorus orbital character of the carbonyl SOMO was verified experimentally<sup>9</sup> by superhyperfine coupling to these nuclei observed in the EPR spectrum of (PNP)Ni(CO). In (PNP)Ni(NO), there are four occupied frontier orbitals that are primarily 3d in character, and the HOMO, shown in

Figure 2c, is heavily nitrosyl  $\pi^*$  (more N than O) and is the counterpart of the lone pair in **A**. The LUMO and LUMO + 1 of both the nitrosyl and the carbonyl<sup>14</sup> are nearly purely the two orthogonal  $\pi^*$  orbitals of the respective diatomic ligands. The only flaw in using the DFT orbitals to deduce the applicable Lewis structure representation **A** is that the  $\angle\text{Ni–N–O}$  is larger than that characteristic of  $sp^2$  nitrogen (generally, bent metal nitrosyls with a lone pair on N have a  $\angle\text{M–N–O}$  less than  $135^\circ$ ). Geometry optimization of the less bulky  $[\text{N}(\text{SiMe}_2\text{CH}_2\text{PMe}_2)_2]\text{Ni}(\text{NO})$  gave<sup>14</sup> no significant change in structure, and especially, the NiNO angle changed by only  $+2.3^\circ$ . The bulk of  $t\text{Bu}$  thus does not control the unusual structural features we discuss here.

Consequently, adding an electron to the SOMO of (PNP)Ni(CO), together with a nuclear proton to the E of NiEO, militates the need for geometric reorganization, specifically bending at E. This is motivated by the antibonding character of the orbital to which the electron is added in (PNP)Ni(CO) to make (PNP)Ni(NO), Figure 2b. Compared to the SOMO of the carbonyl complex, the HOMO of (PNP)Ni(NO) is then a much more strongly amide N lone pair (Figure 2), a localization which reflects the increasingly electron-rich amide character caused by this C-to-N change.

Another view of this is that the nonplanarity of (PNP)Ni leaves its two filled  $\tau_{\text{NiE}}^*$  orbitals nondegenerate, hence, of different back-bonding abilities. The additional electron and nuclear proton at  $E = \text{N}$  finally leads to back-donation sufficiently anisotropic to bend the Ni–N–O angle. Back-bonding is axially symmetric in a rigorously  $C_{3v}$  symmetric  $\text{L}_3\text{Ni}(\text{NO})^+$ .

The intermediate NiNO bend indicates that the choice between (PNP)Ni<sup>+</sup>/NO<sup>−</sup> and (PNP)Ni<sup>−</sup>/NO<sup>+</sup> is a continuum, depending on the reducing power of the (PNP)Ni reagent molecule, and that intermediate (not only integral) degrees of charge transfer are possible, all having singlet spin states. This principle has been deduced previously<sup>15</sup> in NO coordinated to  $\text{RuX}(\text{CO})(\text{PR}_3)_2$ , where X with variable donor power can control  $\angle\text{Ru–N–O}$  and the square-pyramidal/trigonal bipyramidal metal geometry.

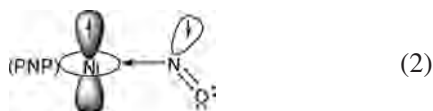
(15) Ogasawara, M.; Huang, D.; Streib, W. E.; Huffman, J. C.; Gallego-Planas, N.; Maseras, F.; Eisenstein, O.; Caulton, K. G. *J. Am. Chem. Soc.* **1997**, *119*, 8642.



Thus,  $C_{3v}$  symmetric  $[\text{MeC}(\text{CH}_2\text{O})_3\text{P}]_3\text{Ni}(\text{NO})^+$  is linear because cationic  $[\text{MeC}(\text{CH}_2\text{O})_3\text{P}]_3\text{Ni}^+$  is not reducing and is in fact oxidizing toward a neutral partner NO. In contrast,  $(\text{PNP})\text{Ni}^+$  is not oxidizing toward neutral reagent NO. Is this due to steric or electronic reasons?

**b. Analogs.** We have probed computationally the above conclusions by relaxing the chelate constraints: DFT(B3LYP) geometry optimization<sup>14</sup> of  $(\text{Me}_3\text{P})_2(\text{Me}_2\text{N})\text{Ni}(\text{NO})$  gives a flattened tetrahedral structure (trans angles  $\text{P}-\text{Ni}-\text{P} = 125.5^\circ$  and  $\text{N}-\text{Ni}-\text{N} = 148.1^\circ$ ) with  $\angle\text{Ni}-\text{N}-\text{O} = 145.5^\circ$ . The chelate does not significantly alter the geometry, which thus reflects the inherent electronic structure of the orbitals involved. If we “turn off” the  $\pi$ -donation of the full PNP amide by protonating that nitrogen,  $[\text{PN}(\text{H})\text{P}]\text{Ni}(\text{NO})^+$  has an optimized geometry with both trans angles equal at  $140.6^\circ$  and a  $\angle\text{NiNO}$  of  $143.8^\circ$ ; thus the geometry is independent of the development of electron density (reducing power) at the metal and apparently derives from the electronic asymmetry of the  $\text{NP}_2$  ligand set.

An open-shell calculation of the triplet state of  $(\text{PNP})\text{Ni}(\text{NO})$  is informative. This yields a small spin density (0.30) on nickel and an unusually large spin density on the nitrosyl N (1.02) and O (0.60). This state has remarkably altered geometry from that of the singlet: planar Ni and strongly bent ( $135.6^\circ$ ) NiNO. These suggest that the triplet state is in fact planar  $\text{Ni}^{\text{II}}$  and  $\text{NO}^-$ , hence  $\text{sp}^2$  hybridized N and an  $\text{sp}^2$ -like  $\angle\text{NiNO}$ , but this is a triplet state relatively localized on  $\text{NO}^-$ . Free  $\text{NO}^-$  has a triplet ground state, of  $(\pi^*)^2$  configuration, and this bonds to planar  $(\text{PNP})\text{Ni}^+$  via one nitrogen lone pair. Consistent with heavier occupancy of the  $\text{NO} \pi^*$  orbital in triplet  $(\text{PNP})\text{Ni}(\text{NO})$  is that it has an NO stretching frequency reduced by  $150 \text{ cm}^{-1}$  from that of the singlet. Together, this indicates that this singlet-to-triplet excitation (this triplet lies  $7.3 \text{ kcal/mol}$  above the singlet ground state) has  $\text{Ni} \rightarrow \text{NO}$  charge transfer character, with triplet  $\text{NO}^-$  coordinated to  $(\text{PNP})\text{Ni}^+$ . This led us to consider the idea that the experimentally observed singlet ground-state is *not*  $(\text{PNP})\text{Ni}^+$  and singlet  $\text{NO}^-$  but, instead, a ground state of the radicals  $(\text{PNP})\text{Ni}$  and  $\text{NO}$ , with their spins coupled by an antiferromagnetic interaction (eq 2). However, an open-shell singlet was calculated to have an energy not significantly lower (lower by  $1.8 \text{ kcal/mol}$ ) than the closed-shell singlet.



The calculated NO stretching frequency was also essentially unchanged between closed shell and the open-shell singlet calculation. Overall then, the conclusion from this study is that the “half-bent” angle cannot be uniquely associated with major spin density on the nitrosyl nitrogen. The other significant changes in the unrestricted triplet state (vs the singlet) are the longer Ni–NO (by  $0.132 \text{ \AA}$ ) and N–O ( $0.033 \text{ \AA}$ ) distances. The change to planar coordination geometry in the triplet, which we use to deduce a +2 oxidation state for nickel, also shows that this planar

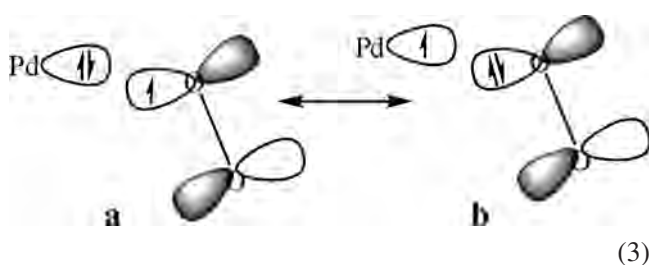
geometry is not dictated by size constraints of the two fused rings of the chelate on Ni but is electronically dictated: both planar and nonplanar coordination geometries can be achieved.

## Discussion

The molecules compared here show complexity beyond what can be described by Lewis structures, since the intermediate NiNO angle fits the extreme of neither  $\text{sp}$  nor  $\text{sp}^2$  hybridization of  $\text{NO}^+$  or  $\text{NO}^-$ , respectively, and the  $143^\circ$  angle is not diagnostic of the more common cause of this angle, where there is high spin density on the nitrogen of a ligand-centered radical.<sup>16–18</sup> Perhaps the contracted d orbitals of a late transition metal leads to weak back-bonding (high Cu(I) carbonyl stretching frequencies<sup>19</sup> show this to be generally true of late transition metals), and consequent poor reducing power toward NO disfavors fully bent ( $\sim 125^\circ$ )  $\text{NO}^-$ . The presence of reduced nitrogen in the half-bent NO group of  $(\text{PNP})\text{Ni}(\text{NO})$  is evident from its easy oxidation to  $(\text{PNP})\text{Ni}(\text{ONO})$  by excess NO.

The low barrier to the planar/nonplanar process that gives the  $^1\text{H}$  NMR a time-averaged  $C_{2v}$  symmetry indicates ready intramolecular redox character due to valence reorganization, or what Enemark and Feltham<sup>2</sup> called “stereochemical control of valence.” Here, since the PNP ligand prohibits reaching a tetrahedral coordination geometry and destroys axial symmetry, the ligand set around nickel leaves the NiNO bend at an intermediate value.

An important comparison case<sup>20</sup> is the geometry of triplet  $\text{O}_2$  approaching  $\text{L}_2\text{Pd}^0$ . This involves a  $d^{10}$   $\text{Pd}^0$  metal center (with a diatomic molecule having two unpaired  $\pi^*$  electrons in contrast to the  $d^9$   $\text{Ni}^{\text{I}}$  and a diatomic molecule with one  $\pi^*$  electron). The  $\text{O}_2/\text{L}_2\text{Pd}$  system shares with  $(\text{PNP})\text{Ni} + \text{NO}$  an approach geometry where only one ligand atom initially interacts, and a frontier orbital interaction represented by eq 3.



Here, the two-orbital/three-electron interaction populates  $\pi_{\text{OO}}^*$  (like  $\text{Ni}^{\text{I}} \rightarrow \text{Ni}^{\text{II}}$  as NO approaches in a nonlinear fashion), clearest in **b**, which represents the *single* electron transfer characteristic to both  $\text{Pd}/\text{O}_2$  and  $\text{Ni}/\text{NO}$  reaction partners. In the Pd case, the second electron transfer (to form

(16) Marchenko, A. V.; Verdenikov, A. N.; Dye, D. F.; Pink, M.; Zaleski, J. M.; Caulton, K. G. *Inorg. Chem.* **2004**, *43*, 351.

(17) Frantz, S.; Sarkar, B.; Sieger, M.; Kaim, W.; Roncaroli, F.; Olabe, J. A.; Zalis, S. *Eur. J. Inorg. Chem.* **2004**, 2902.

(18) Ruggiero, C. E.; Carrier, S. M.; Antholine, W. E.; Whittaker, J. W.; Cramer, C. J.; Tolman, W. B. *J. Am. Chem. Soc.* **1993**, *115*, 11285.

(19) Strauss, S. H. *Dalton Trans.* **2000**, 1.

(20) Landis, C. R.; Morales, C. M.; Stahl, S. S. *J. Am. Chem. Soc.* **2004**, *126*, 16302.

the  $O_2^{2-}$  ligand, which is not relevant to the Ni/NO case) only occurs when the second O begins to interact with Pd.

## Experimental Section

**General.** All reactions were performed in a glovebox or on a Schlenk line using standard air-sensitive techniques. Solvent distillation was carried out using either Na/benzophenone,  $CaH_2$ , 4 Å molecular sieves, and a Grubbs type purification system or a combination of these four. They were degassed and stored in airtight glassware.  $[(Bu_2PCH_2SiMe_2)_2N]NiCl$  and  $[(Bu_2PCH_2SiMe_2)_2N]Ni$  were prepared following the published synthesis.<sup>9</sup>  $^1H$  NMR chemical shifts are reported in parts per million relative to protio impurities in the deuterated solvents.  $^{31}P\{^1H\}$  spectra are referenced to external standards of 85%  $H_3PO_4$  (at 0 ppm). NMR spectra were recorded with a Varian Gemini 2000 (300 MHz  $^1H$ ; 121 MHz  $^{31}P$ ), or a Varian Unity Inova instrument (400 MHz  $^1H$ ; 162 MHz  $^{31}P$ ). Gas reactions were carried out on a calibrated gas line with the solution being first degassed and 2 mL of headspace assumed for the NMR tube.

**$[(Bu_2PCH_2SiMe_2)_2N]NiNO$ .** A total of 15 mg (0.030 mmol) of  $[(Bu_2PCH_2SiMe_2)_2N]Ni$  was placed in 0.5 mL of  $d_8$ -toluene at 25 °C in a J-Young NMR tube. One equivalent of NO was added on a calibrated vacuum line. The solution was warmed to -77 °C, and the color changed from pale yellow to violet. The experiment was repeated in pentane, without allowing the solution to warm to room temperature, and the solvent was then slowly pumped off, through a small orifice, under a dynamic vacuum, to form violet crystals of sufficient quality for the X-ray diffraction study.  $^1H$  NMR (25 °C,  $C_7D_8$ ): 1.12 ppm (d, 36H,  $J_{P-H} = 11.1$  Hz,  $tBu$ ), 0.60 ppm (unresolved doublet, 4H,  $CH_2$ ), 0.56 ppm (s, 12H, SiMe).  $^{31}P\{^1H\}$  NMR (25 °C,  $C_7D_8$ ): 68.3 ppm. IR (pentane,  $cm^{-1}$ ): 1654  $cm^{-1}$ . Excess NO is to be avoided since it converts (PNP)Ni(NO) to an incompletely characterized diamagnetic blue complex, which has equal intensity  $^{31}P\{^1H\}$  NMR signals at 92 (broad) and 74 (doublet,  $J = 9$  Hz) ppm,  $^1H$  NMR doublet peaks at 1.07 and 1.24 ppm, and SiMe singlets at 0.76 and 0.29 ppm; these data allow the compound to be readily distinguished from (PNP)Ni(NO). A second product of excess NO is an orange crystalline solid, identified as (PNP)Ni(ONO) by comparison to an independently synthesized sample, below.

**$[(Bu_2PCH_2SiMe_2)_2N]Ni(ONO)$ .** A total of 15 mg (0.028 mmol) of  $[(Bu_2PCH_2SiMe_2)_2N]NiCl$  was added to 0.5 mL of THF in a J-Young NMR tube. To this was added a large excess (20 equiv) of  $NaNO_2$ , and the solution changed from red to orange over a

24 h period, and  $^{31}P\{^1H\}$  NMR spectra were taken at various times. Conversion: 75% (by  $^{31}P\{^1H\}$  NMR integration).  $^1H$  NMR (25 °C,  $C_6D_6$ ): 1.34 ppm (t, 36H,  $J_{P-H} = 6.4$  Hz,  $tBu$ ), 0.54 ppm (t, 4H,  $J_{P-H} = 5.6$  Hz,  $CH_2$ ), 0.25 ppm (s, 12H, SiMe).  $^{31}P\{^1H\}$  NMR (25 °C,  $C_6D_6$ ): 42.3 ppm.

**Computational Details.** All calculations were carried out using density functional theory as implemented in the Jaguar 5.5 suite<sup>21</sup> of ab initio quantum chemistry programs. Geometry optimizations were performed with the B3LYP<sup>22–25</sup> functional and the 6-31G\*\* basis set with no symmetry restrictions. Nickel was represented using the Los Alamos LACVP basis.<sup>26,27</sup> The energies of the optimized structures were re-evaluated by additional single-point calculations on each optimized geometry using Dunning's correlation-consistent triple- $\zeta$  basis set<sup>28</sup> cc-pVTZ(-f), which includes a double set of polarization functions. For all transition metals, we used a modified version of LACVP, designated as LACV3P, in which the exponents were decontracted to match the effective core potential with the triple- $\zeta$ -quality basis. The models used in this study consist of ~90 atoms, which represent the nontruncated substrates that were also used in the experimental work. These calculations challenge the current state of computational capabilities, and the numerical efficiency of the Jaguar program allows us to accomplish this task in a bearable time frame.

**Acknowledgment.** This work was supported by the National Science Foundation (Grant No. 0544829). M.H.B. is a Cottrell Scholar of the Research Corporation and a Sloan Research Fellow of the Alfred P. Sloan Foundation.

**Supporting Information Available:** Full computational details, together with applicable CIF files and a least-squares fit of (PNP)Ni(NO) to (PNP)Ni(CO). This material is available free of charge via the Internet at <http://pubs.acs.org>.

IC702503M

- 
- (21) Jaguar, 5.5 ed.; Schrodinger, L.L.C.: Portland, OR, 1991–2003.  
 (22) Becke, A. D. *Phys. Rev. A: At., Mol., Opt. Phys.* **1988**, *38*, 3098.  
 (23) Becke, A. D. *J. Chem. Phys.* **1993**, *98*, 5648.  
 (24) Lee, C.; Yang, W.; Parr, R. G. *Phys. Rev. B: Condens. Matter Mater. Phys.* **1988**, *37*, 785.  
 (25) Vosko, S. H.; Wilk, L.; Nusair, M. *Can. J. Phys.* **1980**, *58*, 1200.  
 (26) Hay, P. J.; Wadt, W. R. *J. Chem. Phys.* **1985**, *82*, 270.  
 (27) Wadt, W. R.; Hay, P. J. *J. Chem. Phys.* **1985**, *82*, 284.  
 (28) Dunning, T. H., Jr. *J. Chem. Phys.* **1989**, *90*, 1007.